Signal electronics for an atomic force microscope equipped with a double quartz tuning fork sensor

H.-P. Rust,[a] M. Heyde, and H.-J. Freund
Fritz-Haber-Institut der Max-Planck-Gesellschaft, Faradayweg 4-6, D-14195 Berlin, Germany

(Received 22 December 2005; accepted 15 March 2006; published online 20 April 2006)

Signal electronics equipped with a bandpass filter phase detector for noncontact atomic force microscopy (ncAFM) has been developed. A double quartz tuning fork assembly is used as a force sensor, where one fork serves as a dither tuning fork, while the other is used as a measuring tuning fork. An electrically conductive Pt90Ir10 tip enables the sensor to work in both scanning tunneling microscopy (STM) and AFM modes. Electronic circuits for self-oscillation control and for frequency detection are given in detail. Atomically resolved STM and ncAFM images of a thin alumina film on NiAl(110) are shown with the microscope cooled down to 4.5 K by liquid helium. © *2006 American Institute of Physics.* [DOI: 10.1063/1.2194490]

I. INTRODUCTION

Modern science and technology require sophisticated methods for the investigation of surfaces in real space with the capability of recording images with atomic resolution. Whereas scanning tunneling microscopy is used for electrically conducting or semiconducting samples, atomic force microscopy can be used also for nonconducting samples. Many papers and books describe these two operating principles, e.g., Refs. 1–4.

In constant current scanning tunneling microscopy (STM) operating mode, the tunneling current is kept constant by a control loop, causing the tip to follow the surface contour (local density of states) during the scanning process. The noncontact atomic force microscopy (ncAFM) mode is a little bit more complicated. A tip, attached at the end of a quartz tuning fork, oscillates with a small amplitude in the nanometer range close to the sample surface. The oscillation is driven by a closed electronic circuit loop where the tuning fork's mechanical resonance acts as a frequency normal. The oscillation frequency in this self-oscillation mode changes if the tip-sample interaction force varies. To get topographic surface information, the oscillation frequency is kept constant by a control loop, causing the tip to follow the surface contour with a fixed interaction during the scanning process.

There are a variety of methods for detecting a frequency shift of a tuning fork, such as phase locked loop and countertechniques such as digital methods or diverse analog frequency demodulator circuits. Also commercial hardware is available, e.g., easyPLL.[5] Albrecht *et al.*[6] have used an analog phase demodulator in a frequency modulation (FM) detection system for AFM applications with high Q cantilevers which allows increased sensitivity without restrictions on bandwidth or dynamic range compared with slope or amplitude detection modes. Such phase demodulator circuits are also referred to as Rigger or Foster-Seeley discriminators and were used at the beginning of the last century for radio telegraphy, later for frequency demodulation in audio circuits.

The use of an analog bandpass filter phase detector offers an excellent way of implementing an optimized frequency detection circuit for the operation of a high Q double quartz tuning fork sensor in ncAFM at low temperatures. Design details and technical data of the AFM signal electronics are described in this article. The remarkable performance is shown on several atomically resolved images.

II. EXPERIMENTAL SETUP

Our custom-built STM/AFM microscope is incorporated in an ultrahigh vacuum environment and can be cooled by liquid helium down to 4.5 K (Fig. 1). This experimental design where the microscope head hangs at the end of a stainless steel bellows supported pendulum was originally developed by Weiss and Eigler[7] for STM application. Cooling is performed by helium gas of a pressure of about 10–100 mbars, which makes a heat coupling between the walls of the exchange gas canister which is in contact with the cryogen and the microscope flange.[8]

III. AFM OPERATING ELECTRONICS

Two control loops are needed to run the microscope in ncAFM mode: (1) an oscillation control loop, which stabilizes the amplitude of the tip oscillation, and (2) a z control loop, which holds the frequency of the tuning fork oscillation constant by adjusting the tip to sample distance (Fig. 2). Additionally, a scan control and an approach control unit are needed.

The double quartz tuning fork sensor used here has been described in Ref. 9. Two quartz tuning forks are glued together with a two component epoxy adhesive at an angle of 90° onto the z piezo of the scanner. Here, a slightly modified assembly is used. In the early version, the tip was connected to one electrode of the quartz tuning fork, which could have

[a]Electronic mail: rust@fhi-berlin.mpg.de

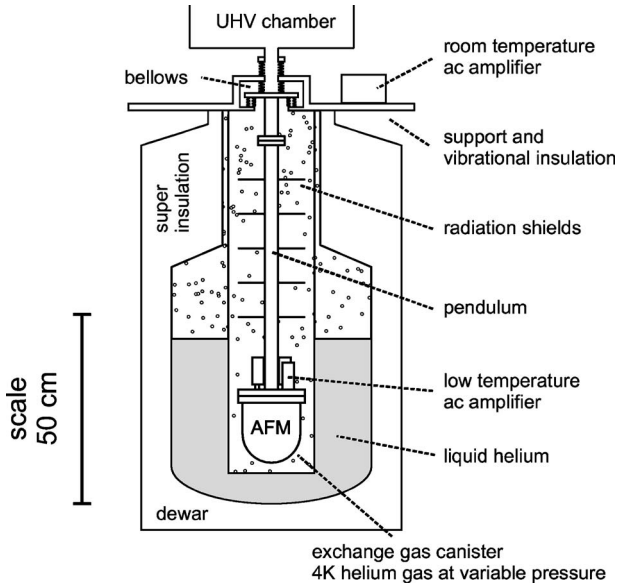

FIG. 1. Schematic of the experimental setup. The pendulum of about 1 m in length is the main design feature for providing mechanical vibrational insulation. At its end, the STM/AFM head is fixed in an ultrahigh vacuum environment while the upper end is suspended from a set of stainless steel bellows. The pendulum is placed inside of a helium gas filled exchange gas canister, which in turn is inserted into liquid helium. The helium gas is cooled by interacting with the walls of the gas canister in contact with the liquid cryogen (nitrogen or helium) and cools the STM/AFM down. The low temperature ac amplifier is placed near the STM/AFM head while the room temperature ac amplifier is placed outside of the Dewar.

caused a coupling between bending of the fork and the tunneling current. We have avoided this influence by gluing a separate tip wire onto the fork.

A. Oscillation control loop

To achieve stable operating conditions for frequency and amplitude of the tuning forks, gain and phase of the oscillation control loop have to be adjusted for a self-oscillating mode. When the measuring tuning fork oscillates, a modulated charge can be measured as an alternating current at its leads with a low temperature ac amplifier (see Fig. 2). To keep the noise low, this amplifier is placed near the AFM sensor (see Fig. 1). The oscillation voltage is then fed into a room temperature amplifier for further amplification. An adjustable phase shifter allows phase and amplification of the loop to be set to a self-oscillation condition. A limiter holds the amplitude constant. To close the oscillation loop, the output signal of the phase shifter is fed back via a voltage divider to the dither tuning fork of the sensor. A fast Fourier transform (FFT) analyzer[10] is used to adjust and monitor the oscillation amplitude. The phase shifter output signal is also fed into the FM detector which is part of the z-control loop. The tuning forks[11] used here have a resonance frequency of $f_0=32.768$ kHz $(=2^{15}$ Hz). The masses of tip, tip current wire, and glue reduce this frequency to about 16.5 kHz. The cutoff frequencies of the oscillation loop components must be higher than this value.

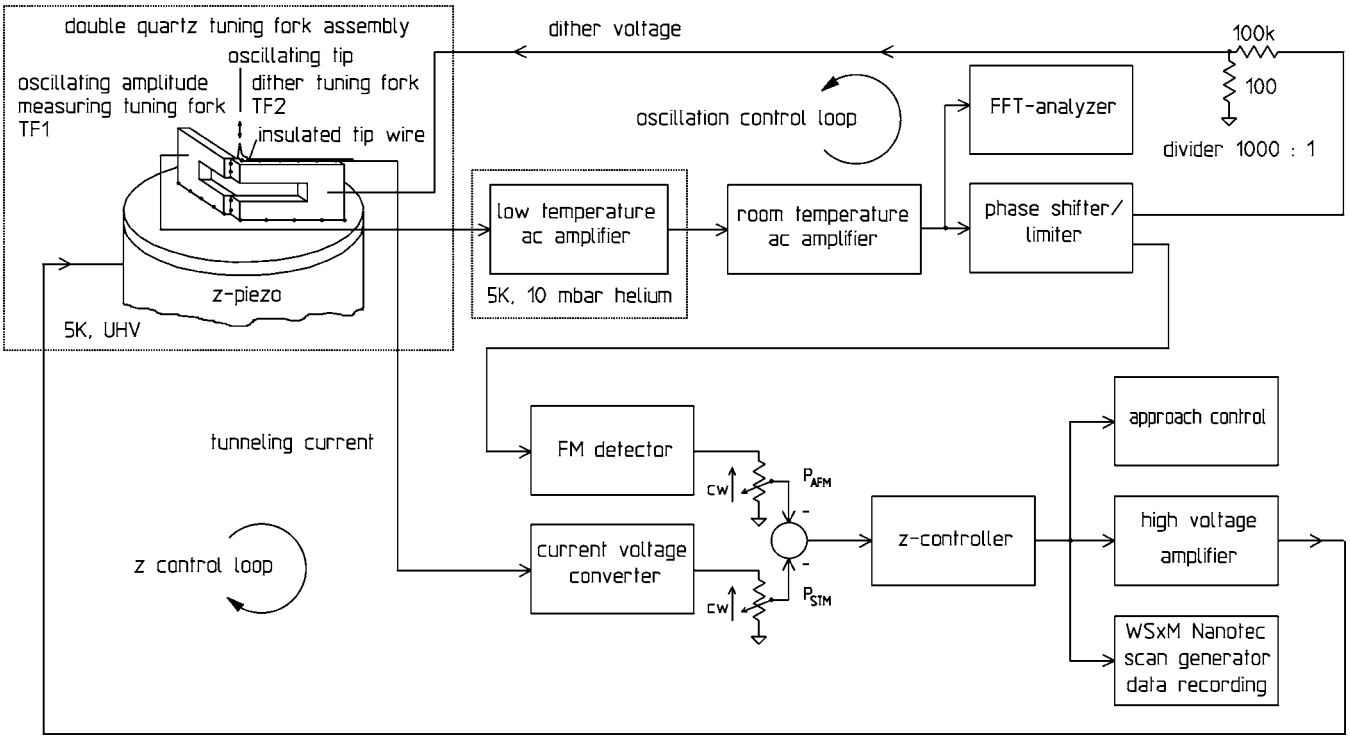

FIG. 2. Electronics block diagram. In the upper part the oscillation control loop for driving the double tuning fork assembly is shown. A low temperature ac amplifier is located near the STM/AFM head. It acts as a preamplifier with an amplification factor of about 10 at 4.5 K. Because of the high Q of about 30 000 of the tuning fork assembly only a small dither voltage amplitude in the order of 1 mV is needed to excite the tuning forks. The sample-tip gap is controlled by the lower control loop. There is one path for STM operation and one path for AFM operation selectable by the two potentiometers.

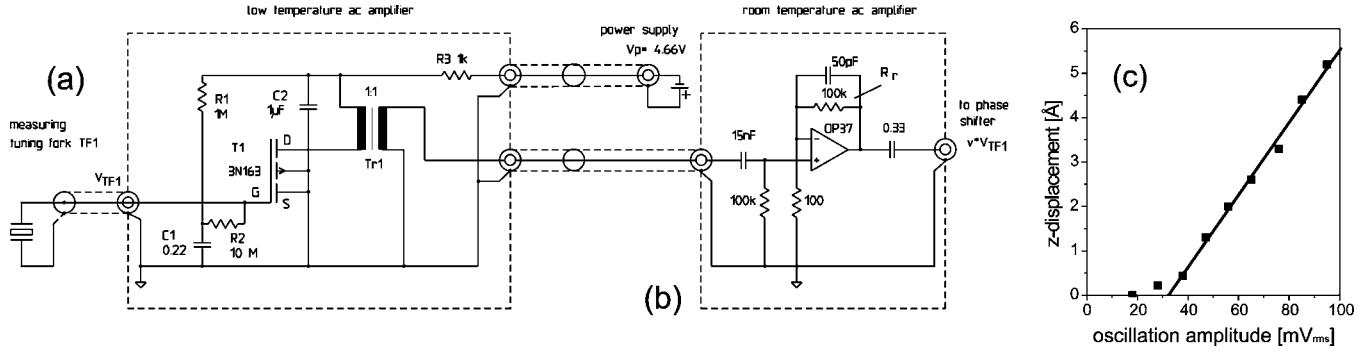

FIG. 3. Oscillation voltage amplifiers and calibration curve. (a) Low temperature amplifier. The amplifier has an input impedance of 10 MΩ and is working at 4.5 K. Its power supply voltage is also used as bias voltage for the *p*-channel MOSFET. *RC* filters (R1/C1 and R3/C2) are incorporated to suppress power line frequencies (50 or 60 Hz). The amplified tuning fork signal is coupled by an audio transformer to the room temperature amplifier. In this circuit, gate-source and drain-source voltages have the same value. (b) Room temperature amplifier. It is a noninverting amplifier with an amplification factor of 1000. The input *RC* filter rejects low frequency noise. (c) Tip-sample displacement as a function of oscillation amplitude when the tunneling current is kept constant by the z-control loop. The slope of the linear part is 0.08 $Å/mV_{rms}$ and is used for calibration of the oscillation amplitude. For lower oscillation amplitude values the *z* displacement does not change, because the mean value of the tunneling current is constant in this region.

1. Oscillation voltage amplifiers

A low temperature amplifier has been designed to convert the charge modulation of the measuring tuning fork into a voltage. A simple room temperature amplifier serves as a second stage (Fig. 3). As mentioned above the low temperature amplifier is located near the AFM sensor on top of the cooled microscope flange outside of ultrahigh vacuum. Because it is necessary for the amplifier to work at the temperature of liquid helium, only *p*-channel enhancement-mode or gallium arsenide metal oxide semiconductor field effect transistors (MOSFETs) can be used. Gallium arsenide MOSFETs are commonly used for gigahertz applications so we have chosen a *p*-channel enhancement-mode MOSFET.[12] The 3N163 transistor has an ultralow input leakage current of typically 0.02 pA at room temperature and is designed for analog switch and preamplifier applications.

The signal from the measuring tuning fork is fed to the gate of the 3N163. The amplified signal is coupled out by a 2 mW audio transformer Tr1 (Ref. 13) (bandwidth of 60 Hz to 25 kHz) and fed into a simple noninverting room temperature amplifier with an amplification factor of about 1000.

Notice that because of their large resistance increase at 4.5 K one cannot use carbon resistors but metal film resistors for the low temperature amplifier.

To calibrate the amplifiers, the microscope and the low temperature amplifier were cooled down to 4.5 K. The tip was placed over a clean and atomically flat metal surface in constant current STM mode where the tip-surface gap is in the order of a few angstroms. An external dither voltage generated by a lock-in amplifier[14] drives the tuning fork assembly at its resonance frequency. The dither voltage amplitude was increased slowly from zero while the output voltage of the room temperature amplifier was monitored by the FFT analyzer.

The mean value of the relative tip-sample *z* displacement in angstroms was determined by measuring the variation of the *z* piezovoltage. At low amplitudes where the tip oscillates in the 1 Å range the tunneling current is modulated by the tip motion but in this case the mean tip-sample distance is the same as in the pure STM mode. At larger oscillation amplitudes a tunneling current flows only when the tip comes near the sample surface—the mean value of the now pulse shaped tunneling current is kept constant by the STM controller—and the tip-sample distance rises almost linearly with the oscillation amplitude [Fig. 3(c)]. The gradient for amplitudes larger than 40 mV gives a sensitivity of 0.08 $Å/mV_{rms}$. This value will be used later to adjust the oscillation amplitude for ncAFM operation. Notice that in Fig. 3(c) the *z* displacement is a relative value. At zero oscillation amplitude set point the tuning fork is not oscillating and the tip-sample distance is kept constant by the STM controller.

2. Phase shifter/limiter

To keep the sensor in a self-oscillating mode the phase shift of the oscillation control loop has to be set to 180°, and the loop amplification to unity. The output signal of the room temperature amplifier is fed to the input of the phase shifter/limiter (Fig. 4) and ac coupled to the instrumentation amplifier A1. The amplification factor of A1 is adjustable continuously between 2 and 100 by P1 or can be set fixed to 1 or 10 to cover different input amplitudes. For a typical input voltage amplitude of about 80 mV_{rms} the amplification factor was set to 20. The phase can be adjusted with the four following phase shift stages. Each stage has a maximal shift range of 120°, so a range of 480° can be adjusted continuously by the four 10-turn potentiometers without any switches. This is very convenient for the adjustment procedure because a phase switching can cause the tip to crash into the sample.

A stable oscillation amplitude for the tuning fork is reached in a very simple way. The two diodes D1 and D2 parallel to the output line limit the peak amplitude. As a result the ac amplification factor is scaled down. With potentiometers P1 and P2 a stable oscillation condition of constant amplitude can be set. It is necessary to mention that for sensor dissipation measurements this simple limiter circuit is not sufficient. In such a case, an additional amplitude controller has to be added.

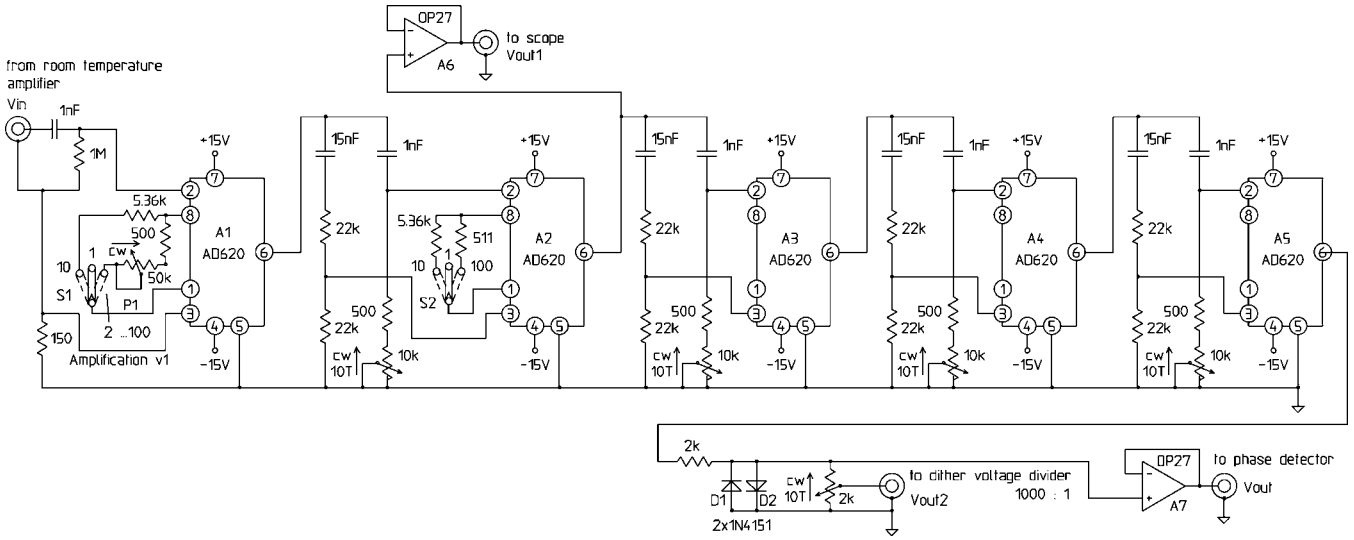

FIG. 4. Phase shifter/limiter. The phase of the tuning fork oscillation signal can be shifted by four *RC* bridges continuously by 480 while the amplitude is kept constant. The four bridges are separated by instrumentation amplifiers. Three outputs are available, output one for monitors the oscillation voltage, output two drives the dither tuning fork, and output three is connected with the phase detector input.

B. The *z*-control loop

After the tip has been brought near the surface by the microscope's coarse approach the distance between tip and sample is controlled by the z piezo. Two pathways can be selected by potentiometers P_{AFM} and P_{STM} (see Fig. 2). By setting P_{STM} fully clockwise (cw) and P_{AFM} fully counterclockwise (ccw), the control loop runs via tip-sample distance (tunneling current), tip current to voltage converter, z controller, high voltage amplifier, and z piezo. No special electronics is used here. The current to voltage conversion factor and the cutoff frequency can be switched. The z controller is a custom-built analog unit with an adjustable proportional and integral path. The AFM operating mode is selected by setting the P_{STM} fully ccw and P_{AFM} fully cw. The signal flows now from the measuring tuning fork (frequency), ac low temperature and room temperature amplifiers, phase shifter/limiter, FM detector, z controller, and high voltage amplifier to the z piezo. In this loop the frequency detector plays an important part and will be explained in detail. The continuously variable cross fade between the two operating modes is an advantage so as to avoid tip crashes. Also, a mixed AFM/STM operation is possible, allowing for adjustment of the time constants for stable operating conditions while cross fading slowly from one operation mode to the other one. For scanning and recording images, commercially available hardware and software have been used.[15]

1. The FM detector

The principal item used here for detecting a frequency modulation is an analog bandpass filter phase detector circuit (Fig. 5), shown as a detailed circuit in Fig. 6.

The ac coupled input signal drives the instrumentation amplifier A1 into its saturation leading to an amplitude stabilization of the amplifier's trapezoidal shaped output voltage. This voltage is divided by a factor of 100 and drives the bandpass filter composed of two parallel resonance circuits (C1A, C1B, L1 and C2A, C2B, L2) coupled by the capacitor Ck. Because of the capacitor's tolerances, C1 and C2 are split in two capacitors each for a better matching procedure. The value of Ck can be selected by a switch. A modulation of the input frequency causes a phase modulation between the voltages V_{LC1} and V_{LC2}. The following comparator circuits amplify and convert the sinusoidal voltages to pulse voltages and scale the amplitudes down to complementary metal oxide semiconductor (CMOS) circuit levels. The two NAND gates then form the pulse width modulated output voltage V_{PW}, which has to be converted into a dc voltage. A simple *RC* low pass filter converter is not used here because the output voltage of the NAND gate varies with ambient temperature and supply voltage. The better way is to convert the pulse width by a digital to analog converter (DAC) into a voltage as shown in Fig. 6. V_{PW} is given to the most significant bit of the AD667JN DAC,[16] while the other bits are

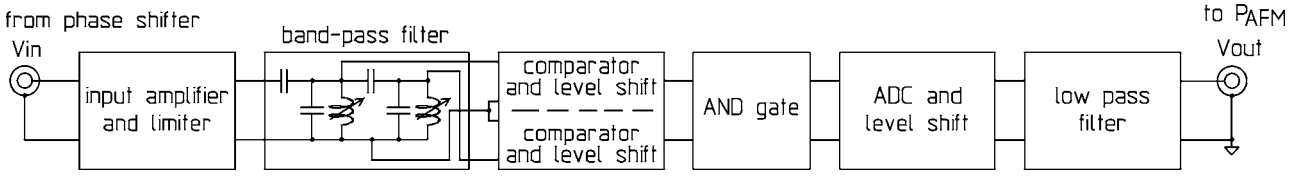

FIG. 5. Block diagram of the FM detector. The input voltage is amplified and limited to a maximum value in the first stage for driving the bandpass filter with a constant amplitude. Two 90° phase shifted sinusoidal output signals from the bandpass filter are converted to rectangular voltages and compared in a logical AND gate. The now pulse width modulated AND gate output signal is converted to a precision analog voltage by a digital to analog converter. An adjustable low pass filter is necessary for a stable operation of the z-control loop.

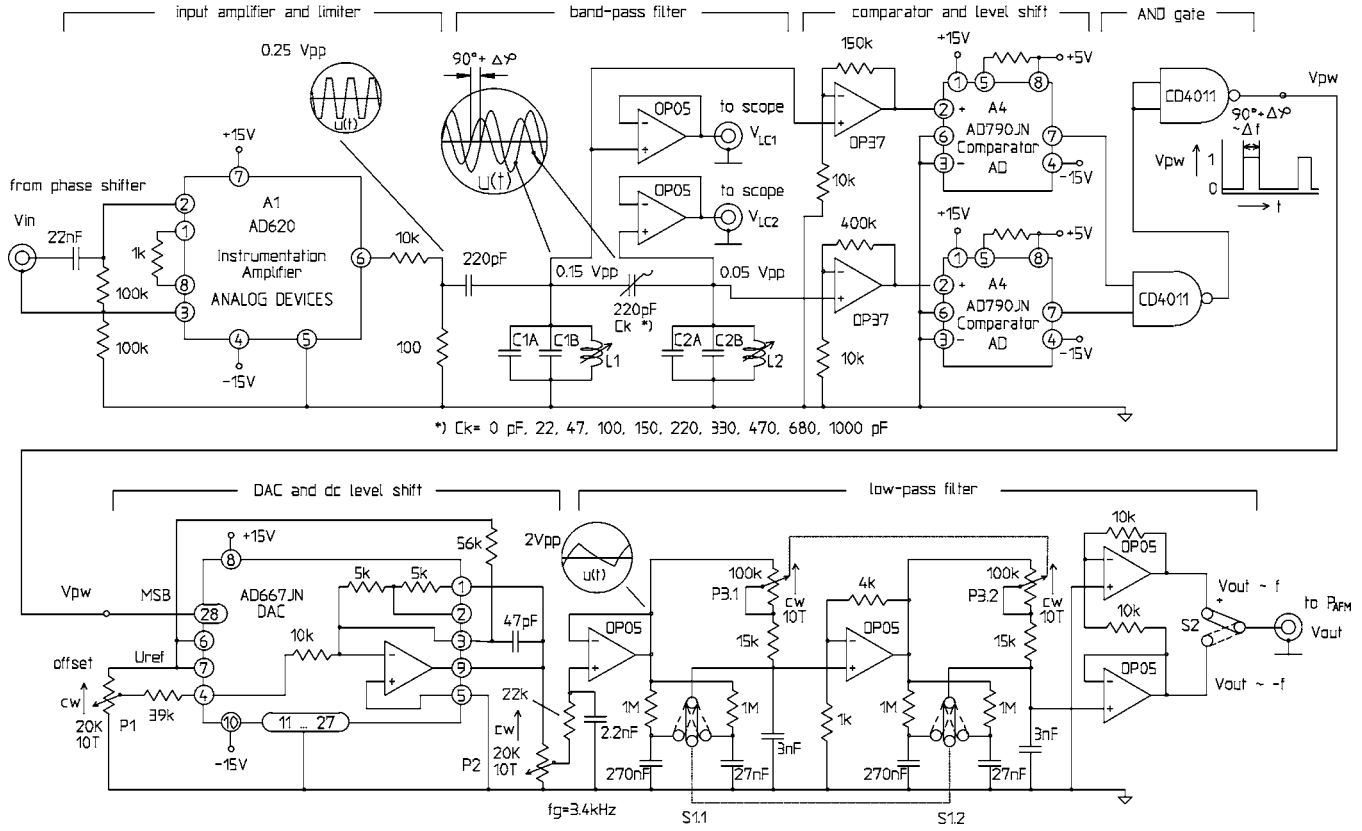

FIG. 6. FM detector circuit. The input voltage drives the instrumentation amplifier A1 slightly into saturation, as shown in the scope image inset. The two filter voltages can be monitored by a dual beam oscilloscope connected to two OP05 amplifier buffered outputs. The tuning of the bandpass filter will be explained in the next chapter. The OP37 amplifier together with the AD790 comparator acts as a sinusoidal to rectangular converter. The OP37 is needed to overcome the offset error of the AD790. Two NAND gates act as an AND gate which drives the 12 bit DAC. The temperature stability is determined by the zero offset drift of about ±5 ppm of FSR/°C. The scope inset shows the filtered DAC output voltage. This voltage is filtered by two *RC* filters with an adjustable cutoff frequency between 5 Hz and 3.6 kHz. The output voltage is adjusted to zero with the potentiometer P1 for the undamped resonance frequency of the tuning fork. The slope of the output voltage as a function of frequency shift is set by S2.

grounded. The DAC creates a pulsed output voltage and its mean value is proportional to the pulse width of the input voltage. The dc level of the output voltage can be shifted with P1 by feeding an adjustable current into the DAC's operational amplifier. A first *RC* low pass filter stage with a cutoff frequency of about 3 kHz is implemented by the 22 $k\Omega$/2.2 nF components which smoothes the DAC's pulse shaped output voltage. Two more low pass filter stages with adjustable cutoff frequency are implemented. The cutoff frequency can be set by S1 and P3 from about 5 Hz to 3.6 kHz. The polarity of the output voltage can be selected by S2 to set the right phase in the *z*-control loop.

2. Testing the FM detector

Before measuring the specifications of the FM detector the resonance circuits have to be tuned. A voltage of 0.5 V_{rms} generated by a lock-in amplifier[14] with the resonance frequency of the double tuning fork is fed to the input. The resonance circuit voltages are monitored by a dual beam oscilloscope. Ck is set to 0 pF to make the coupling between the resonance circuits zero. The first circuit is tuned to a maximum voltage by adjusting the ferrite core of the inductance L1.[17] Then Ck is increased to 220 pF where the resonance circuits are slightly under critically coupled. Then L2 is tuned to adjust the phase shift between the voltages V_{LC1} and V_{LC2} to 90°. Now, the sensitivity of the FM detector can be checked by increasing and decreasing the frequency of the input voltage by 1 Hz. This gives a sensitivity of 66 mV/Hz and 0.015 Hz/mV, respectively.

The long term dc stability depends essentially on the temperature coefficient of the *L* and *C* components of the bandpass filter. Therefore we use multilayer ceramic capacitors[18] which have a temperature coefficient of ±30 $\times 10^{-6}$/K. The capacitors and inductances have been thermally isolated to slow down temperature changes. The thermal coefficient of the FM detector is about 20 mV/K. This leads to a long term dc stability in a normal air conditioned laboratory environment of better than 10 mV/h and 0.15 Hz/h, respectively.

The noise of the output voltage depends on the cutoff frequency of the low pass filter. The cutoff frequency should be set to the lowest possible value where the control loop can still work stably The output noise is 0.3 $\mathrm{mV_{rms}}$ or 0.0045 Hz for the lowest cutoff frequency of 5 Hz.

IV. EXPERIMENTAL RESULTS

The STM/AFM head was tested in STM mode for calibration of the *x*, *y*, and *z* piezo constants. In Fig. 7(a) monatomic steps of the Cu(100) surface were used for *z*-voltage

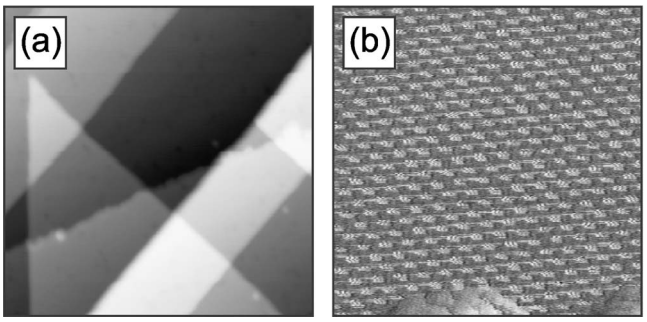

FIG. 7. Constant current STM images of a Cu(100) surface. (a) Overview shows atomic flat terraces, 420×420 Å^2, $V_S=200$ mV, and $I_T=0.1$ nA. (b) Atomically resolved terrace, 47×47 Å^2, $V_S=10$ mV, and $I_T=10$ pA.

calibration, while from the atomic distances in Fig. 7(b) the x and y distances and also the distortion were extracted to calibrate the x and y voltages.

After it was clear that the double tuning fork assembly was working stably in the STM mode, ncAFM experiments were carried out on a thin alumina film grown on a NiAl(110) crystal. Oxide films are of great industrial interest especially for heterogeneous catalysis.[19–23] Alumina grows on the NiAl(110) surface in two domains, each rotated by 22.7 grad against the [1-10] direction of the NiAl(110). The domains exhibit a periodical structure with a unit cell size of 10.5×17.9 Å^2 [see Fig. 10(b)]. The preparation procedure for the oxide can be done in such a way that the NiAl(110) surface is only partially covered by the alumina film. So, measurements can be made on both the bare metal surface and the alumina film.

At first, on the metallic NiAl(110) surface, the frequency shift of the tuning fork as a function of sample bias voltage was measured at a fixed tip-sample distance [Fig. 8(a)]. The tuning fork was excited in the self-oscillation mode with an amplitude of about 5 Å. The electrostatic force between tip and sample increases quadratically with the bias voltage and causes a frequency shift shown in Fig. 8(a). As the curve is symmetric there is no cross talk between tunneling current and frequency shift. A crosstalk would bend the left and the right hand part of the curve in opposite directions.

To determine a frequency shift to tip-sample distance curve, the tuning fork was also excited in the self-oscillation mode with the amplitude set to about 5 Å. The tip was placed at a fixed position above the alumina surface and the z controller was switched off. The z distance between the tip apex and the surface was chosen to be large enough so that no frequency shift was detected. To record the frequency shift as a function of z displacement the tip was slowly moved towards the surface and back to the starting point by a z-piezovoltage ramp [Fig. 8(b)]. When the tip approaches the surface, attractive forces cause a negative frequency shift. As the tip moves closer to the surface, repulsive forces become stronger, driving the frequency shift in a positive direction. The curve goes to a minimum and then to positive values. Figure 8(b) shows a typical curve with a frequency shift from zero to a minimum value of about 6 Hz. This value can become larger or smaller and depends on the configuration of the tip. For AFM image recording, a frequency shift from -1.5 to -3 Hz in the repulsive or attractive region is recommended for this oxide film. It should be mentioned here that such a spectrum looks completely different for a metallic surface. Therefore, special care has to be taken when recording ncAFM images on samples where a metallic surface is only partly covered with an oxide film.

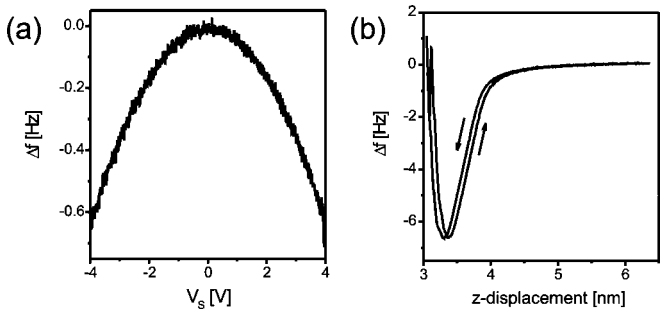

FIG. 8. Frequency shift of the tuning fork sensor. (a) Frequency shift as a function of sample bias voltage measured on a NiAl(110) surface. (b) Frequency shift as a function of tip-sample displacement measured on the thin alumina film. The hysteresis is caused by a tip change at high repulsive forces.

In a second step we used also the thin alumina film to record STM and AFM images (Fig. 9). Figure 9(a) shows a raw data STM image where at a sample voltage of 27 mV atomic resolution is achieved. The power spectrum [Fig. 9(b)] and the autocorrelation function [Fig. 9(c)] show the periodic structure as well as size and direction of the alumina unit cell. High frequency noise was filtered out of Fig. 9(a) by Fourier filtering and the filtered image is shown in Fig. 9(d). Image processing was done with the WSXM software.[24]

NcAFM images were taken on the same alumina film as used in Fig. 9(a). A raw data image is shown in Fig. 9(e), which looks noisier compared with the STM image in Fig. 9(a). To test whether there is detailed information on the alumina film in the image, the power spectrum [Fig. 9(f)] and the autocorrelation function [Fig. 9(g)] have been calculated. The power spectrum shows space frequencies up to 0.5/Å as bright spots, higher frequencies are not visible. The autocorrelation function [Fig. 9(g)] shows clearly the unit cell of the film. To remove noise from the image, Fig. 9(e) was Fourier low pass filtered by masking out all the frequencies larger than 0.7/Å. The filtered image [Fig. 9(h)] shows more clearly the periodic structure of the alumina film. The resolution of the image in Fig. 9(e) is not high enough to determine the atom positions of the topmost layer of the alumina film. Therefore, a high resolution image was recorded [Fig. 10(a)].

The structure of the alumina film has been resolved recently by density functional theory calculations and STM experiments.[25] Based on this model, the surface layer contains 28 oxygen atoms which form square and rectangular features and 24 aluminum atoms arranged in a nearly hexagonal pattern. The height difference between the surface aluminum layer and the surface oxygen layer is 0.40 Å whereas the aluminum layer is nearer to the bulk.

We noticed in our AFM images periodically arranged black spots, which correspond to lower topographic sites. For a better visibility, we have inverted the contrast so that the lower topographic sites are shown as bright spots [Fig.

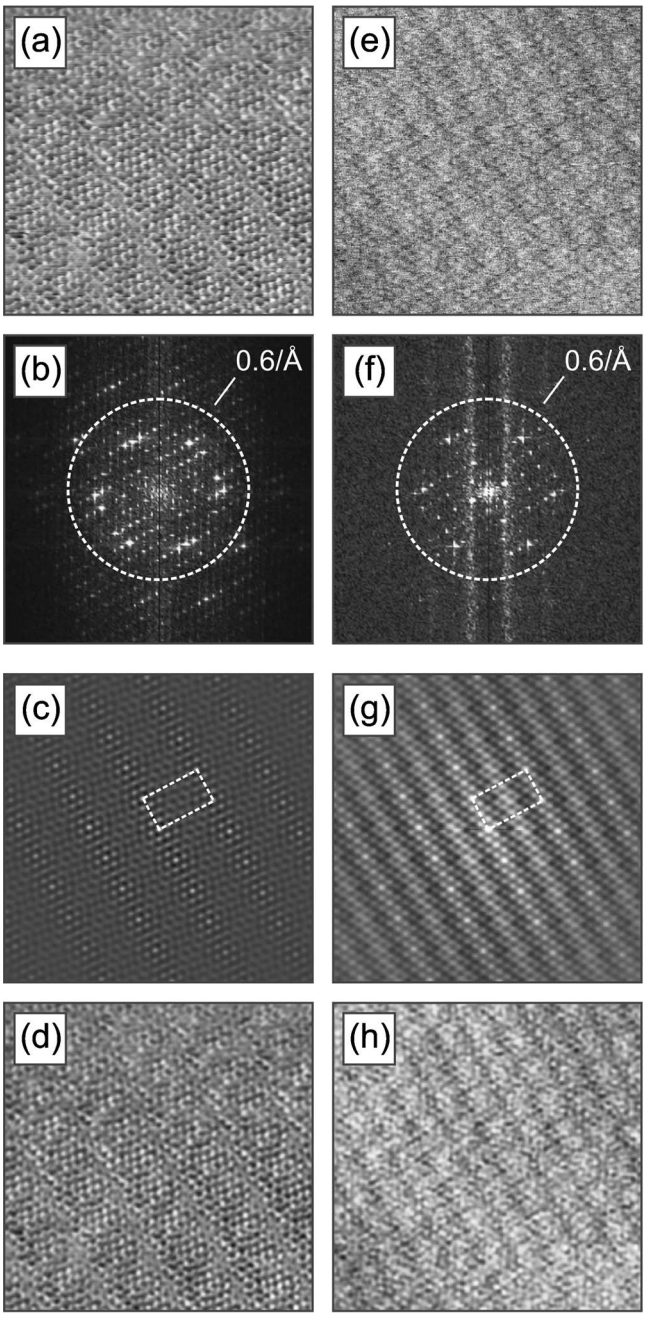

FIG. 9. STM and ncAFM images of the thin alumina film on NiAl(110), 85×85 Å^2, and $T=4.5$ K. (a) Constant current STM image, $V_S=27$ mV, and $I_T=64$ pA. (b) Power spectrum of (a). (c) Autocorrelation function of (a) showing size and direction of the 10.5×17.9 Å^2 alumina unit cell. (d) Low pass filtered image. (e) ncAFM raw data image, $\Delta f=-1.5$ Hz, and repulsive region, $V_S=0$ V. (f) Power spectrum of (e). (g) Autocorrelation function of (e) also showing size and direction of the alumina unit cell. (h) Low pass filtered image.

10(a)]. Three unit cells and the atoms (bright spots) therein have been marked in the same way as in Ref. 25. The two zigzag lines delimit the 10.5×17.9 Å^2 unit cells. By comparing now the bright spots in our image with the surface layer aluminum atoms in the Kresse model, we found also 24 atoms in one unit cell and they form a nearly hexagonal pattern as described for the model. Therefore, we assign the bright features in Fig. 10(a) to aluminum atoms of the surface layer. It is not the aim of this article to discuss on a theoretical base the tip-sample interactions which are responsible for the image contrast. This will be done in a separate article.

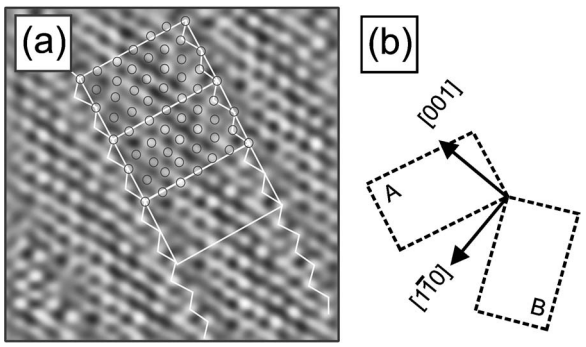

FIG. 10. (a) AFM image (50×50 Å^2 of a thin alumina film grown on a NiAl(110) crystal, domain A, $V_S=0$ V, $\Delta f=-3$ Hz, $T=4.5$ K, low pass filtered, and contrast inverted: bright, lower topographic sites, dark, higher topographic sites. Three unit cells 10.5×17.9 Å^2 and the atom positions in two unit cells have been marked. (b) Schematic of the alumina unit cells with respect to the NiAl(110) direction.

V. DISCUSSION

The developed electronics offers a practical way to record ncAFM images with atomic resolution. The sensitivity is sufficient to run a quartz tuning fork sensor with a regular Q factor of about 10 000 in UHV at 4.5 K. There is some room left for improvements. Amplitude stabilization of the phase shifter can be replaced by an amplitude controller for dissipation measurements. The low temperature amplifier should be replaced by a differential amplifier to improve the signal to noise ratio of the tuning fork oscillation amplitude. The ferrite solenoid should be shielded against magnetic fields. Keeping the temperature of the bandpass filter components constant by a thermostat would increase the long term stability of the output voltage.

ACKNOWLEDGMENTS

The authors take pleasure in thanking Niklas Nilius, Thomas P. Pearl, Maria Kulawik, and Georg Heyne for very fruitful discussions and suggestions.

[1] G. Binnig, H. Rohrer, C. Gerber, and E. Weibel, Phys. Rev. Lett. **50**, 120 (1983).
[2] F. J. Giessibl, Science **267**, 68 (1995).
[3] K. S. Kitamura and M. Iwatsuki, Jpn. J. Appl. Phys., Part 2 **34**, L145 (1995).
[4] H. J. Hug, B. Stiefel, P. J. A. van Schendel, A. Moser, S. Martin, and H.-J. Güntherodt, Rev. Sci. Instrum. **70**, 3625 (1999).
[5] Nanosurf AG, Grammetstrasse 14, CH-4410 Liestal, Swiss, 2005.
[6] T. R. Albrecht, P. Grütter, D. Horne, and D. Rugar, J. Appl. Phys. **69**, 668 (1991).
[7] P. S. Weiss and D. M. Eigler, in *Nanosources and Manipulations of Atoms under High Fields and Temperatures: Applications*, NATO Advanced Studies Institute, Series E: Applied Science, edited by V. T. Binh, N. Garcia, and K. Dransfeld (Plenum, New York, 1993), Vol. 235.
[8] H.-P. Rust, M. Doering, J. I. Pascual, T. P. Pearl, and P. S. Weiss, Rev. Sci. Instrum. **72**, 4393 (2001).
[9] M. Heyde, M. Kulawik, H.-P. Rust, and H.-J. Freund, Rev. Sci. Instrum. **75**, 2446 (2004).
[10] SR770 FFT network analyzer, Stanford Research Systems, Inc., 1290-D Reamwood Avenue, Sunnyvale, CA 94089, 2005.
[11] Quartz 304-447, RS Components GmbH, Hessenring 13b, D-64546

Mörfelden-Walldorf, Germany, 2004.
[12] 3N163, Vishay Electronic GmbH, Geheimrat-Rosenthal-Str. 100, D-95100 Selb, Germany, 2003.
[13] Audio Transformer, Part No. 210-6380, RS Components GmbH, Hessenring 13b, D-64546 Mörfelden-Walldorf, Germany, 2005.
[14] 7260 DSP lock-in amplifier, EG&G Instruments, 2004.
[15] WSXM hardware, Nanotec Electronica S.L., Centro Empresarial Euronova 3, 28760 Tres Cantos, Madrid, Spain, 2005.
[16] 12-Bit D/A converter AD667JN, Analog Devices, Inc., P.O. Box 9106, Norwood, MA 02062-9106, 2005.
[17] Ferrite component RM6, Part No. 29-733-41, RS Components GmbH, Hessenring 13b, D-64546 Mörfelden-Walldorf, Germany, 2005.
[18] COG multilayer ceramic capacitor, EPCOS Inc., 186 Wood Avenue South, Iselin, NJ 08830, 2005.
[19] C. T. Campbell, Space Sci. Rev. **27**, 1 (1997).
[20] H.-J. Freund, Faraday Discuss. **114**, 1 (1999).
[21] M. Bäumer and H.-J. Freund, Prog. Surf. Sci. **61**, 127 (1999).
[22] M. Kulawik, N. Nilius, H.-P. Rust, and H.-J. Freund, Phys. Rev. Lett. **91**, 256101 (2003).
[23] W. T. Wallace, B. K. Min, and D. W. Goodman, Top. Catal. **34**, 17 (2005).
[24] WSXM Nanotec Electronica S.L., Centro Empresarial Euronova 3, 28760 Tres Cantos, Madrid, Spain, 2005. Free software downloadable at http://www.nanotec.es
[25] G. Kresse, M. Schmid, E. Napetschnig, M. Shishkin, L. Köhler, and P. Varga, Science **308**, 1440 (2005).